

# Biodegradable chitin conduit tubulation combined with bone marrow mesenchymal stem cell transplantation for treatment of spinal cord injury by reducing glial scar and cavity formation

Feng Xue<sup>1,#</sup>, Er-jun Wu<sup>2,#</sup>, Pei-xun Zhang<sup>1,#</sup>, Li-ya A<sup>1</sup>, Yu-hui Kou<sup>1,\*</sup>, Xiao-feng Yin<sup>1,\*</sup>, Na Han<sup>3,\*</sup>

1 Department of Trauma and Orthopedics, Peking University People's Hospital, Beijing, China

2 Graduate School of Shanxi Medical University, Taiyuan, Shanxi Province, China

3 Central Laboratory, Peking University People's Hospital, Beijing, China

## \*Correspondence to:

Na Han, Ph.D., 876804705@qq.com.

Yu-hui Kou, Ph.D., kouyuhui@163.com.

Xiao-feng Yin, Ph.D.,

xiaofengyin@bjmu.edu.cn.

#These authors contributed equally to this work.

doi:10.4103/1673-5374.150715

<http://www.nrronline.org/>

Accepted: 2014-12-10

## Abstract

We examined the restorative effect of modified biodegradable chitin conduits in combination with bone marrow mesenchymal stem cell transplantation after right spinal cord hemisection injury. Immunohistochemical staining revealed that biological conduit sleeve bridging reduced glial scar formation and spinal muscular atrophy after spinal cord hemisection. Bone marrow mesenchymal stem cells survived and proliferated after transplantation *in vivo*, and differentiated into cells double-positive for S100 (Schwann cell marker) and glial fibrillary acidic protein (glial cell marker) at 8 weeks. Retrograde tracing showed that more nerve fibers had grown through the injured spinal cord at 14 weeks after combination therapy than either treatment alone. Our findings indicate that a biological conduit combined with bone marrow mesenchymal stem cell transplantation effectively prevented scar formation and provided a favorable local microenvironment for the proliferation, migration and differentiation of bone marrow mesenchymal stem cells in the spinal cord, thus promoting restoration following spinal cord hemisection injury.

**Key Words:** nerve regeneration; spinal cord injury; spinal cord hemisection; biological conduit; bone marrow mesenchymal stem cells; stem cells; transmission electron microscope; cell transplantation; neurons; nerve fibers; NSFC grants; neural regeneration

**Funding:** This study was supported by grants from the National Program on Key Basic Research Project of China (973 Program), No. 2014CB542201; Program for Innovative Research Team in University of Ministry of Education of China, No. IRT1201; the National Natural Science Foundation of China, No. 31271284, 31171150, 81171146, 30971526, 31100860, 31040043; Program for New Century Excellent Talents in University of Ministry of Education of China, No. BMU20110270; the Natural Science Foundation of Beijing of China, No. 7142164.

Xue F, Wu EJ, Zhang PX, ALY, Kou YH, Yin XF, Han N (2015) Biodegradable chitin conduit tubulation combined with bone marrow mesenchymal stem cell transplantation for treatment of spinal cord injury by reducing glial scar and cavity formation. *Neural Regen Res* 10(1):104-111.

## Introduction

A variety of cells, such as bone marrow mesenchymal stem cells (BMSCs), Schwann cells, olfactory ensheathing cells and neural stem cells, are potentially suitable seed cells for the repair of spinal cord injury (Guest et al., 1997; Lu et al., 2003; Patist et al., 2004; Tsai et al., 2004; Jia et al., 2014; Liu et al., 2014).

In preliminary studies, we developed completely biodegradable chitin conduits to be used as biological scaffolds, which showed promising results in the restoration of peripheral nerve injury *in vivo* (Zhang et al., 2008, 2009, 2011, 2013). To minimize surgical complications after spinal cord injury, we modified our biodegradable chitin conduits, replacing the sleeve-joint model with a point-like suture model after chitin sleeve placement. Here, we observed the microenvironment

around the injured spinal cord after biological conduit tubulation and BMSC transplantation, to evaluate the combined efficacy of the two treatments in the restoration of the spinal cord after injury, using immunohistochemistry, transmission electron microscopy and retrograde tracing.

## Materials and Methods

### Experimental animals

Sixty-one healthy 3-month-old male Sprague-Dawley rats weighing  $300 \pm 15$  g, and two male rats expressing green fluorescent protein (GFP) and weighing  $200 \pm 25$  g (used for the preparation of BMSC suspension), all specific pathogen-free, were provided by the Academy of Military Medical Sciences of China (license No. SCXK (Jing) 2013-0001). Experiments were approved by the Ethics Committee of Peking University

People's Hospital of China (approval No. 2013-055).

### Chitin conduits

The conduit was a hollow cylindrical sleeve of chitin (deacetyl chitin; China Textile Academy, Beijing, China; patent No. 0113631412), 4 mm in length, 1 mm thick, with an internal diameter of 3 mm.

### *In vitro* culture of rat BMSCs

The femur, tibia and ilium of the two rats expressing GFP were harvested under sterile conditions. Bone marrow mesenchymal stem cells were rinsed, and a single cell suspension was prepared and slowly seeded onto Dulbecco's modified Eagle medium containing 20% fetal bovine serum, at a density of  $1.5 \times 10^5/\text{cm}^2$ . After 24 hours of culture, adherence characteristics of the BMSCs were determined, the cells were subcultured, and non-adherent cells were removed. Passage 3 BMSCs showing good growth were used for transplantation. BMSC morphology was observed in 24-well plates under an inverted fluorescence microscope (Leica DMI3000B, Heidelberg, Germany) when the culture reached  $6 \times 10^5/\text{cm}^2$ . BMSCs at  $6 \times 10^6/\mu\text{L}$  were used for cell transplantation (Zhang et al., 2005).

### Establishing a rat model of spinal cord injury

Sixty rats were anesthetized with an intraperitoneal injection of 2% sodium pentobarbital (40 mg/kg body weight). The T<sub>8</sub> and T<sub>9</sub> spinous processes and vertebral plates were exposed and the right vertebral plate was removed, exposing the dura. Once the midline was identified, the right spinal cord was transected at T<sub>8/9</sub> to establish the spinal cord hemisection injury model. Sixty rat models were established successfully, and randomly divided into three groups: injury group (spinal cord hemisection was produced, with no subsequent treatment); biological chitin tube (BCT) group (after hemisection, the biological conduit was wrapped around the spinal cord, then the conduit sleeve was sutured to the anterior spinal cord); and a BCT combined with BMSC transplantation (BCT + BMSC) group (after hemisection, 5  $\mu\text{L}$  of passage 3 BMSC suspension was microinjected into the distal end of the injury site (Zhang et al., 2005), followed by suturing of the conduit sleeve). Each group contained 20 rats. One naïve Sprague-Dawley rat was used as a control. In the injury group and BCT groups, spinal cord specimens were harvested from two rats at 2 weeks and from six rats at 4, 8 and 14 weeks; in the BCT + BMSC group, spinal cord specimens were harvested from two rats at 1 day, 5 days, 1 week, and 2 weeks, and from three rats at 4, 8 and 14 weeks (Zhang et al., 2005).

### Hematoxylin-eosin staining

Spinal cord tissue was harvested, fixed in 4% paraformaldehyde, and subjected to a series of procedures, including wax immersion, embedding, paraffin sections, grilling, dewaxing, gradient ethanol dehydration, transparency, and mounting. Spinal cord sections were observed under a DFC 300FX microscope (Leica).

### Immunofluorescence staining

Spinal cord (30 mm in length) was harvested and divided

into three segments: a 10-mm injury segment, comprising 5 mm of spinal cord either side of the hemisection site; and 10-mm segments immediately either side of the injury segment. The cord was fixed in 4% paraformaldehyde, and immersed in 15% and 30% sucrose solution at 4°C overnight, embedded in optimal cutting temperature compound, and cut into frozen sections (7  $\mu\text{m}$  thick). Sections were fixed in acetone at -20°C for 20 minutes, rinsed with 0.3% Triton X-100 (Hyclone, Logan, Utah, USA) in PBS three times, for 5 minutes each time, and blocked with 10% normal goat serum (Hyclone) for 1 hour. The sections were incubated with mouse anti-rat glial fibrillary acidic protein (GFAP) monoclonal antibody and S100 monoclonal antibody (1:200; Abcam, Cambridge, UK) overnight at room temperature, rinsed with 0.3% Triton X-100/PBS three times for 5 minutes each time, and tritinated. Finally, the sections were incubated with goat anti-mouse Cy3 monoclonal antibody (1:200; Abcam) at room temperature for 1 hour, and rinsed again with 0.3% Triton X-100/PBS three times, without antigen retrieval, before mounting. Cells expressing both GFAP and S100 fluoresced red. The migration of BMSCs in each group of spinal cord sections was examined under a fluorescence microscope (Leica DMI3000B), and their survival and differentiation were observed under a confocal laser scanning microscope (type C2, Nikon, Tokyo, Japan) (Zhang et al., 2013).

### Electron microscope observations

Ultrathin sections (70 nm) obtained from the injury site and surrounding spinal cord tissue were observed under a transmission electron microscope (Philips CM 120, Amsterdam, the Netherlands) at 2 weeks (short-term repair) and 14 weeks (long-term repair) and counterstained with saturated uranyl acetate solution for 20 minutes and lead citrate for 10 minutes.

### Biotin dextran amine (BDA) retrograde tracing and development

Rats in the injury and BCT groups were microinjected with 2  $\mu\text{L}$  of 10% BDA solution, 3 mm lateral to the injury site, 2 and 14 weeks postoperatively. Spinal cord specimens were harvested 10 days after injection, and were divided into three segments, as described for immunofluorescence staining. The brain and spinal cord tissues were harvested and incubated in PBS containing 0.05% diaminobenzidine and 0.03% H<sub>2</sub>O<sub>2</sub> (Hyatt et al., 2014); BDA-positive cells were identified by brown staining.

### Statistical analysis

Measurement data were expressed as the mean  $\pm$  SD and the groups were compared by one-way analysis of variance and the least significant difference test, using SPSS 13.0 software (SPSS, Chicago, IL, USA).  $P < 0.05$  was considered statistically significant.

## Results

### Morphology of rat BMSCs

GFP transgenic rats provide stable, fluorescently labeled

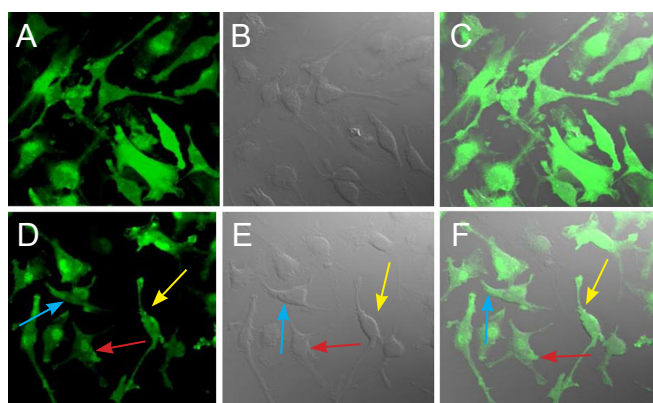


**Figure 1 Morphology of passage 3 bone marrow mesenchymal stem cells (BMSCs) expressing green fluorescent protein (fluorescence microscopy, × 200).**  
 (A–C) Morphology of passage 3 BMSCs; (D–F) three forms of BMSCs: fusiform (yellow arrow), polygonal (blue arrow), and flat irregular (red arrow). (A, D) Green fluorescence emitted by BMSCs; (B, E) transmitted light microscopy of BMSCs; (C, F) merge of autofluorescence and transmitted light images. The subcultured BMSCs were evenly distributed and fusiform shaped. Both primary cultured and subcultured BMSCs expressed green fluorescent protein, the cells emitted bright green fluorescence, and nuclei emitted the strongest fluorescence.

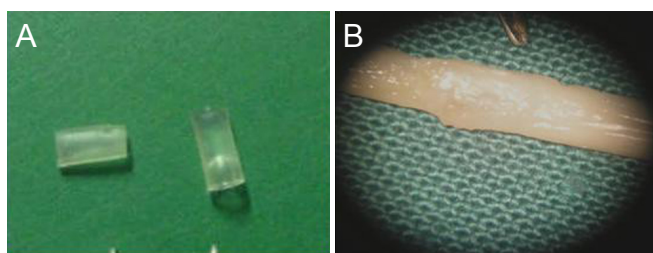


**Figure 2 Spinal cord at 14 weeks after hemisection and biological chitin conduit placement.**  
 (A) Two chitin conduits; (B) conduit in place over the spinal cord. There was notably less glial scar formation at the injury site in the biological chitin tube group compared with the injury group. Spinal cord segments were well connected to the conduit and the thickness of the spinal cord was uniform.

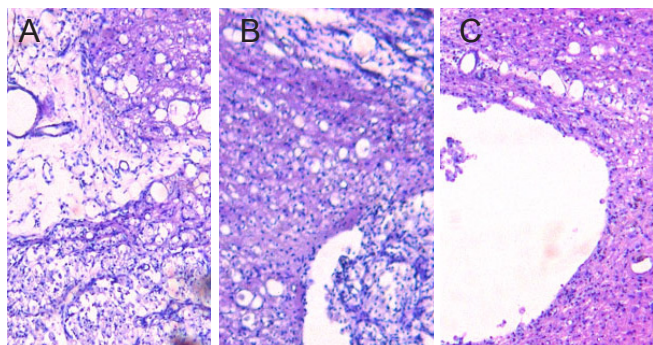


**Figure 3 Spinal cord cavity at the injury site 8 weeks after spinal cord injury (hematoxylin-eosin staining, optical microscopy, × 100).**  
 (A) Injury group; (B) BCT group; (C) BCT + BMSC group. Eight weeks after surgery, there was noticeably less scarring at the injury site than after 1 week. The BCT group (B) and BCT + BMSC group (C) had smaller cavities than the injury group (A). Hyperplastic tissue was noted in the BCT + BMSC group (C). BCT: Biological chitin tube; BMSC: bone marrow mesenchymal stem cell.

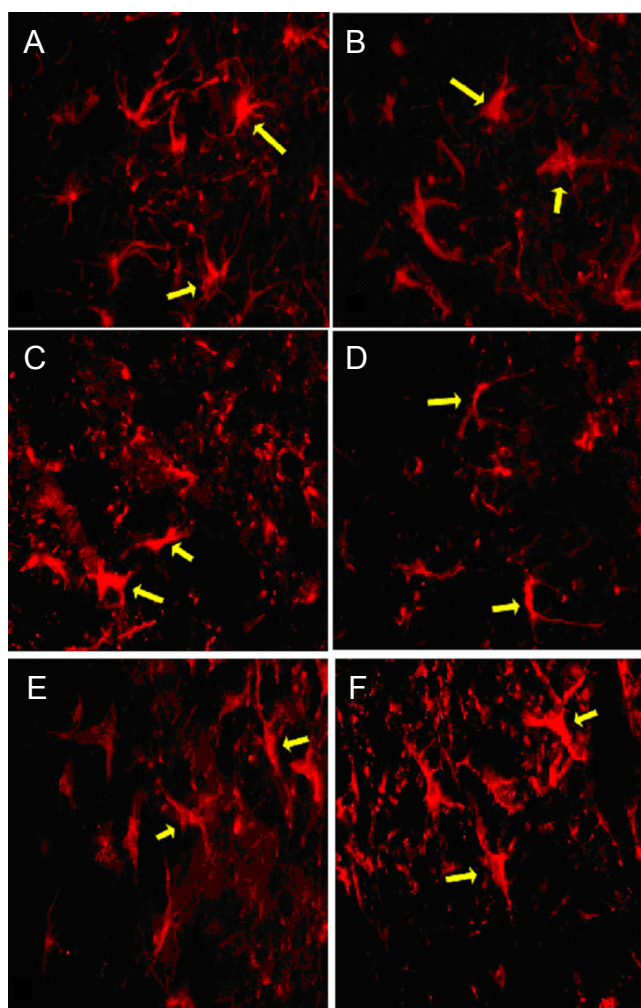


**Figure 4 Morphology of astrocytes at the injury site, 2 and 8 weeks after spinal cord hemisection (immunofluorescence staining, fluorescence microscopy, × 400).**  
 (A–D) Two weeks after injury: Morphology of astrocytes at the proximal (A) and distal (B) ends of the injury segment in the biological chitin tube group, and at the proximal (C) and distal (D) ends of the injury segment in the injury group. (E–F) Eight weeks post-injury, astrocyte morphology was similar in the biological chitin tube (E) and injury (F) groups. Astrocytes remained visible but with smaller cell bodies and lighter staining than in previous weeks. Arrows refer to astrocytes expressing glial fibrillary acidic protein.

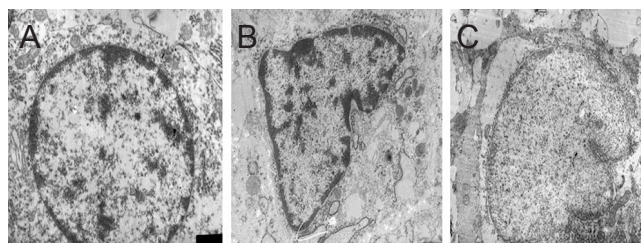


**Figure 5 Morphology of spinal cord neurons at hemisection sites after insertion of the biological conduit and transplantation of bone marrow mesenchymal stem cells (transmission electron microscope, × 10,000).**  
 (A) Normal neurons with intact organelles; (B) apoptotic neurons in spinal cord tissue of the BCT group 2 weeks after surgery; (C) neurons in the BCT + BMSC group showed deformed nuclei, condensation, and loss of cytoplasmic contents 2 weeks after surgery. BCT: Biological chitin tube; BMSC: bone marrow mesenchymal stem cell.

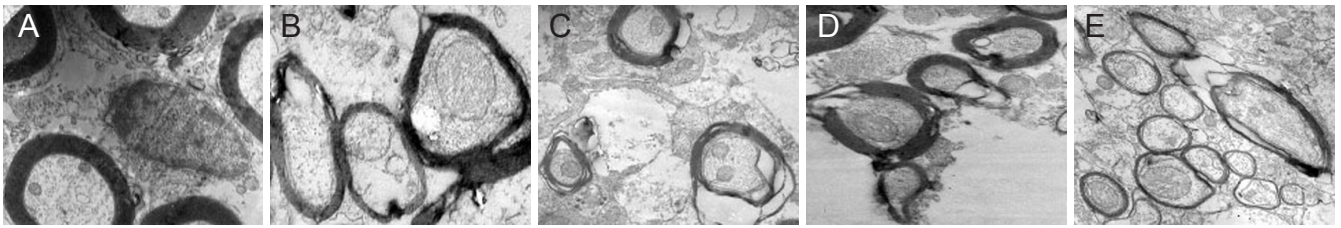


**Figure 6 Morphology of the myelin sheath at the spinal cord hemisection site (transmission electron microscope, × 10,000).**

(A) Normal myelin with uniform thickness; (B) biological chitin tube group, 2 weeks after surgery, showing slight myelin disintegration; (C) injury group, 2 weeks after surgery, showing considerable myelin disintegration; (D) biological chitin tube group, 14 weeks after surgery, showing coexisting regenerated and disintegrated myelin; (E) injury group, 14 weeks after surgery, showing some myelin regeneration.

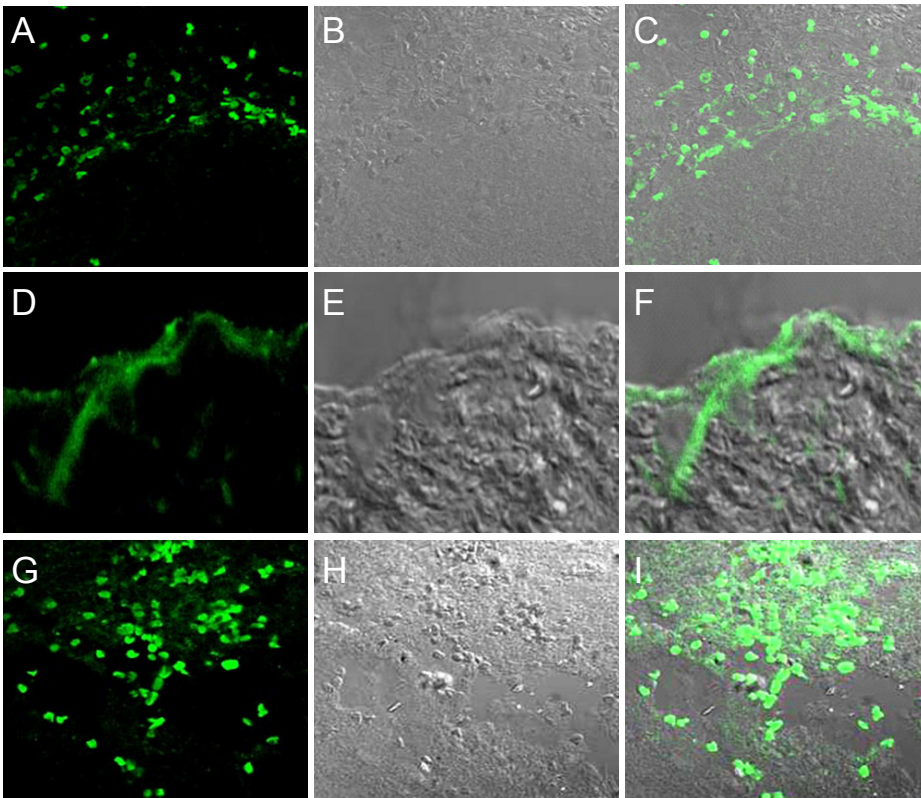


**Figure 9 Migration and distribution of bone marrow mesenchymal stem cells (BMSCs) in the spinal cord of rats in the biological chitin tube + BMSC group (× 40).**

At 1 day (A–C) and 4 weeks (D–F) after BMSC transplantation, BMSCs were localized in the distal end of the injury site; (G–I) at 8 weeks, however, BMSCs were distributed in the proximal end of the spinal cord to the injury. (A, D, G) fluorescence microscopy; (B, E, H) transmitted light; (C, F, I) merged images. As the environment within the spinal cord changed, BMSCs migrated from the distal end to the proximal end.

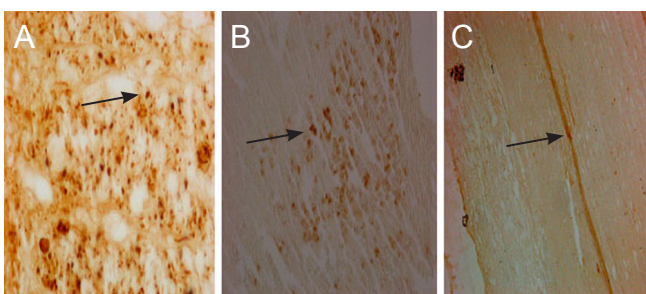


**Figure 7 Neuronal retrograde tracing and nerve fibers at the spinal cord hemisection injury site after combined biological conduit (biotin dextran amine staining, light microscope).**

(A) Morphology of normal cerebral cortex (× 400); (B) morphology of cerebral cortex in the biological chitin tube group 14 weeks after surgery (× 200), showing biotin dextran amine-positive fibers, terminals and cells in the contralateral side to the injection site; (C) strongly labeled spinal cord nerve fibers in the biological chitin tube group 14 weeks after surgery against a pale yellow background, showing a clear distinction between labeled fibers and terminals (× 100). Arrows refer to biotin dextran amine-positive cells.

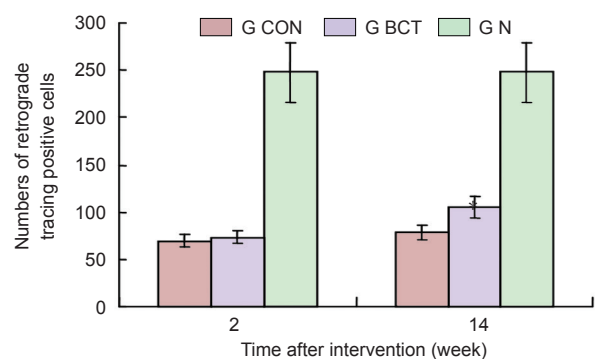


**Figure 8 Quantification of biotin dextran amine-positive neurons at spinal cord hemisection site after retrograde tracing.**

G CON: injury group ( $n = 20$ ); G BCT: biological chitin tube group ( $n = 20$ ); G N: normal control group ( $n = 1$ ). Two weeks after surgery, no difference was observed in biotin dextran amine-positive cell number between the injury and BCT groups. By 14 weeks, significantly more biotin dextran amine-positive cells were found in the BCT group than in the injury group ( $*P < 0.01$ ; one-way analysis of variance and the least significant difference test). Data are expressed as the mean  $\pm$  SD.

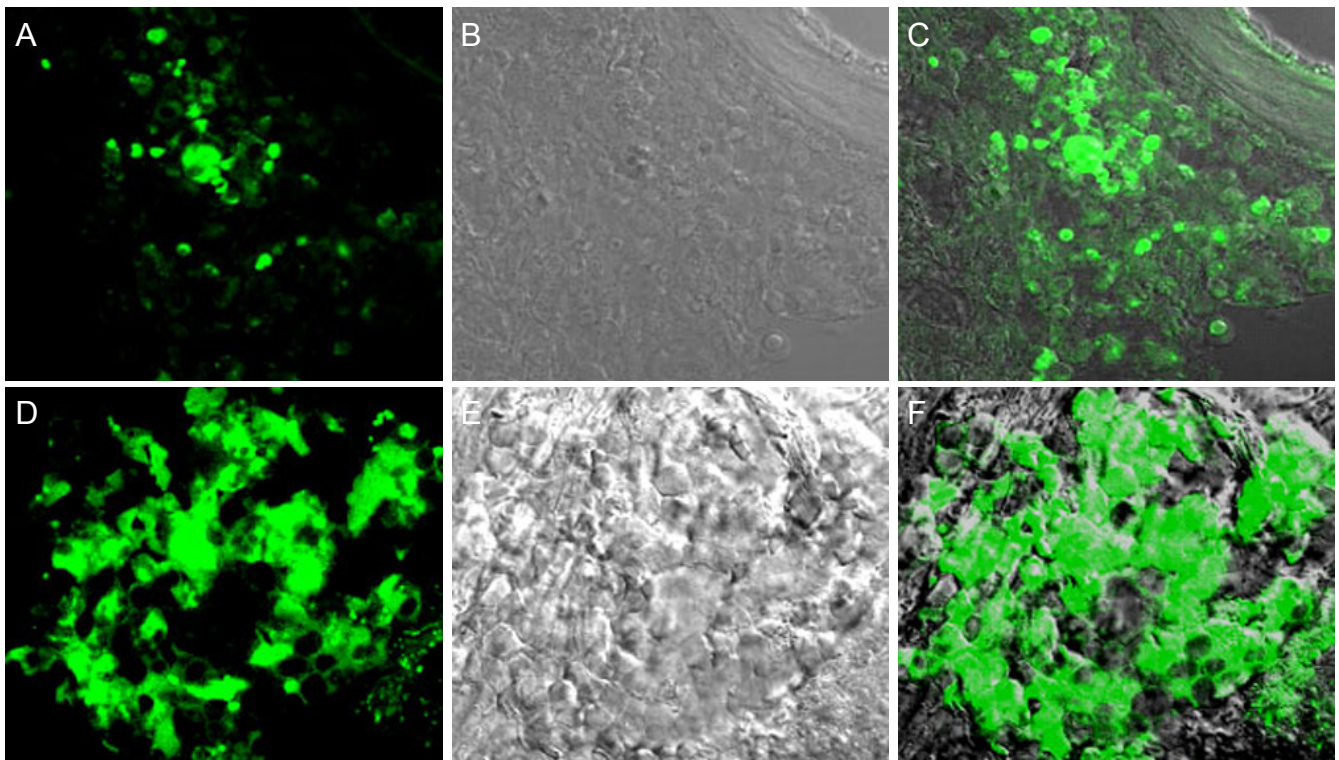


**Figure 10** Growth of bone marrow mesenchymal stem cells (BMSCs) within the rat spinal cord (biological chitin tube + BMSC group) (fluorescence microscopy,  $\times 40$ ).

(A–C) Day 5 after BMSC transplantation; (D–F) a large number of BMSCs proliferated at 8 weeks after BMSC transplantation. (A, D) fluorescence microscopy; (B, E) transmitted light microscopy; (C, F) merged.

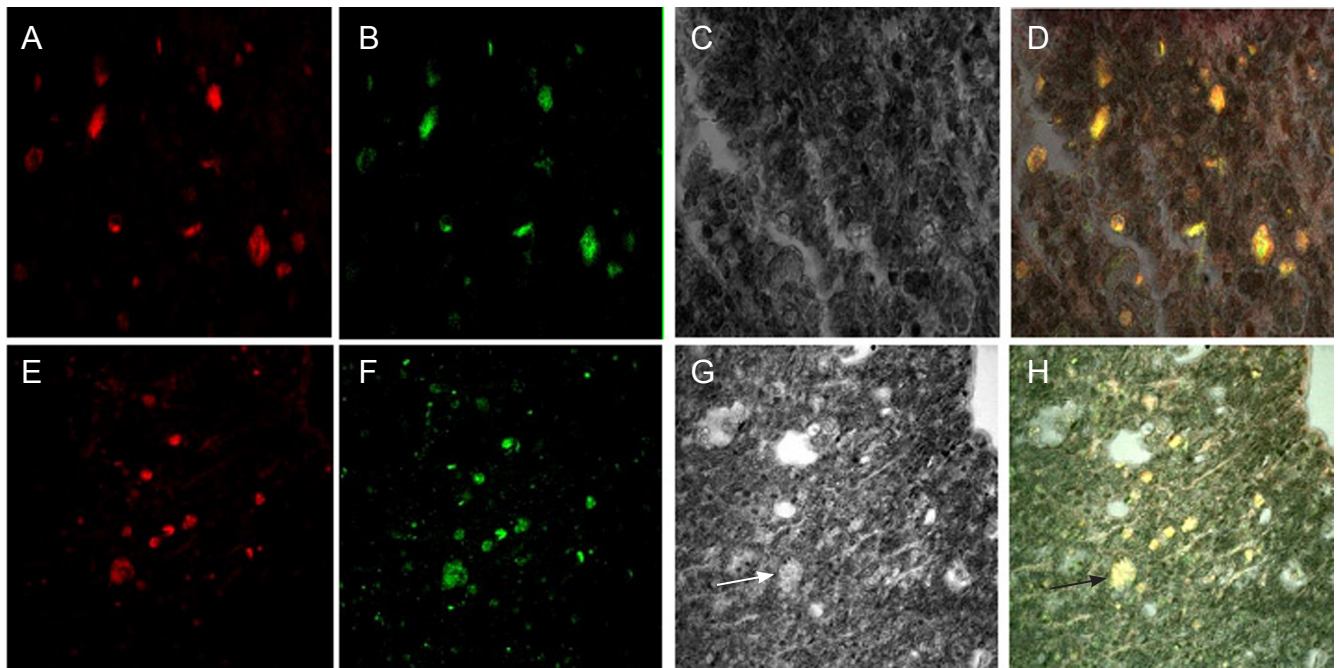


**Figure 11** Confocal microscopy of bone marrow mesenchymal stem cells (BMSCs) showing their differentiation into Schwann cells (S100 phenotype) at 8 weeks after BMSC transplantation (BCT + BMSC group) ( $\times 400$ ).

(A–D) Distal end of the spinal cord injury site; (E–H) proximal end of the spinal cord injury site. (A, E) Red fluorescence, S100-positive staining; (B, F) green fluorescence, BMSC autofluorescence; (C, G) transmitted light irradiation; (D, H) merged images of red, green, and transmitted light. Arrows refer to Schwann cells (S-100 phenotype).

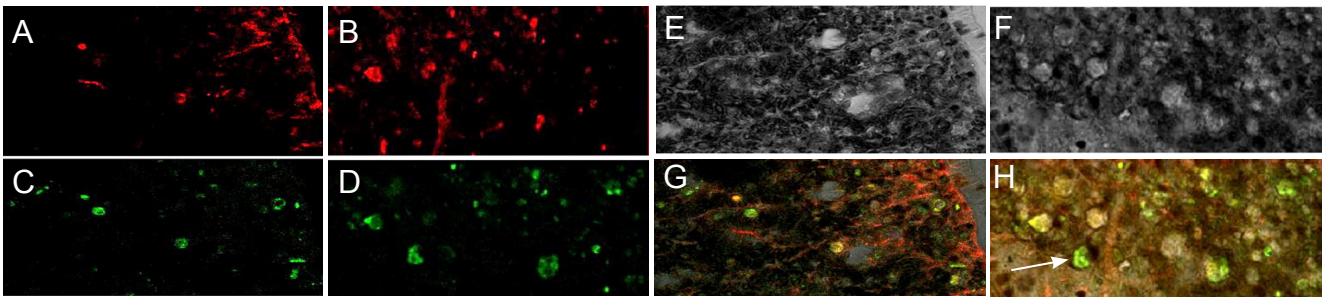


**Figure 12** Differentiation of bone marrow mesenchymal stem cells (BMSCs) into astrocyte-like cells 8 weeks after BMSC transplantation (immunofluorescence staining, laser confocal microscopy,  $\times 400$ ).

(A–D) Distal end of the spinal cord injury site; (E–H) proximal end of the spinal cord injury site. (A, E) Red fluorescence, glial fibrillary acidic protein (GFAP) staining; (B, F) green fluorescence, BMSC autofluorescence; (C, G) transmitted light microscopy; (D, H) merged images of red, green, and transmitted light.

cells. In the present study, primary cells mainly formed colonies, and had fusiform fibroblast-like morphology. Both primary and subcultured BMSCs expressed GFP (Figure 1).

#### Morphology of the injured spinal cord

At 14 weeks after surgery, the injured spinal cord appeared smooth and rounded in the groups that received the biological chitin conduit (Figure 2).

#### Histological changes at spinal cord hemisection site after combined biological conduit and BMSC treatment

Hematoxylin-eosin staining of the injury group showed that, 1 week after surgery, gray matter structures were completely destroyed, neuronal structure had collapsed, and a cavity had formed in the central injury area (Figure 3). A large number of inflammatory cells, particularly macrophages, were observed around the injury site. Eight weeks after surgery, the area of scarring around the injury site was smaller than after 1 week. In the BCT and BCT + BMSC groups, the cavity was notably smaller than that in the injury group. Hypertrophic tissue was observed in the BCT + BMSC group.

Astrocytes were observed using GFAP staining at 2 and 8 weeks (two rats per time point) after spinal cord injury. GFAP-positive cells were scattered among normal spinal cord gray and white matter, with small cell bodies and small cell protrusions. GFAP-positive cells were not distributed in the central injury area, but were arranged symmetrically at the distal and proximal ends of the injury site. One week after injury, reactive astrocytes were hypertrophic and gathered at the edge of the injury site, forming a scar at the boundary of normal and injured spinal cord tissue. GFAP immunofluorescence in astrocytes peaked 2 weeks after injury (Figure 4A–D); at this time, there were a large number of GFAP-positive cells in the central injury area, showing cell body hypertrophy and elongated projections connected to a dense network, leading to the lesion cavity. By 8 weeks post-injury, astrocyte morphology was similar between the injury and BCT groups (Figure 4E–F); astrocytes remained visible, but the cell bodies were smaller than in previous weeks and the staining was lighter.

#### Ultrastructural changes at spinal cord hemisection injury sites after combined biological conduit and BMSC treatment

Transmission electron microscopy revealed intact organelles, normal morphology, clear Nissl bodies and intact cell membranes in normal neurons 2 weeks after surgery (Figure 5A). Apoptotic neurons (Figure 5B, C) showed degeneration, deformed nuclei, and loss of cytoplasmic contents, characteristics typical of cells undergoing apoptosis.

Two weeks after surgery (Figure 6), normal myelin was uniform in thickness and appeared as a dense lamellar-like structure. However, in the injury group, myelinated nerve fibers showed notable axonal shrinkage due to Wallerian degeneration; the gap between axonal neurites and the myelin sheath had increased, electronic density was greater and myelin disintegration had occurred as a result of axonal degeneration. By 14 weeks, some new myelin had formed in the injury group. In the BCT group, 2 weeks after surgery, the myelin sheath had disintegrated, but at 14 weeks, healthy and degenerated myelin coexisted (Figure 6).

#### Morphology of nerve fibers at the spinal cord hemisection site after combined biological conduit and BMSC treatment

BDA retrograde tracing results revealed that fibers from the corticospinal tract projected to cortical pyramidal cells (Figure 7). Two weeks after surgery, the number of BDA-positive cells was similar between the injury and BCT groups, whereas at 14 weeks, more BDA-positive cells were found in the BCT group than in the injury group ( $P < 0.01$ ; Figure 8). This indicated that the biological sleeve conduit effectively promoted the growth of axonal neurites through the injured area.

#### In vivo migration, proliferation and differentiation of BMSCs

At the early stage after BMSCs transplantation into the distal end of the spinal cord injury site, a large number of cells aggregated in the BCT + BMSC group, largely at the edge of the spinal cord tissue (Figure 9A–F). However, at 8 weeks, BMSCs were distributed around the spinal cord in the BCT + BMSC

group and grew into the site of injury (Figure 9G–I). This indicated that, along with the changing environment within the spinal cord, BMSCs migrated from the distal end to the proximal end.

In the BCT + BMSC group, at each time point (from 1 day to 8 weeks) after BMSC transplantation (Figure 10), BMSCs spontaneously emitted fluorescence, and proliferated at 8 weeks.

At 8 weeks after BMSC transplantation (BCT + BMSC group), S100, a specific marker protein of Schwann cells, was used to counterstain BMSCs. Although no S100-immunopositive cells were found in the *in vitro* cultured BMSCs before transplantation, 8 weeks after transplantation, all BMSCs expressed S100 (Figure 11), indicating that all the BMSCs had differentiated into Schwann cells.

In the BCT + BMSC group, at 8 weeks after BMSC transplantation, the astrocyte-specific marker protein GFAP was used to counterstain BMSCs. BMSCs expressed GFAP (Figure 12A, E), while no GFAP phenotype was observed in the *in vitro* cultured BMSCs before transplantation, indicating that BMSCs differentiate into astrocyte-like cells *in vivo*.

## Discussion

The capacity of nerve regeneration after spinal cord injury is limited by various factors, including apoptosis, regenerative power, local microenvironment, and glial scar formation (Mohammadian et al., 2013; Oliveri et al., 2014; Yin et al., 2014). Spinal cord tissue is fragile, anatomically deep, and is prone to liquefactive necrosis after injury, which hinders recovery. In a previous study, we developed a completely biodegradable chitin sleeve conduit with good outcomes in the repair of peripheral nerve injury (Zhang et al., 2005). The sleeve conduit effectively blocked the invasion of external fibrous connective tissue and maintained a local microenvironment conducive to regeneration.

To date, few studies have investigated the application of biological sleeve conduits in the treatment of spinal cord injury (Teng et al., 2002; Sundback et al., 2003). In the present study, we modified the suture technique for biological conduits, from sleeve-joint suture to point-shaped suture, and adopted the conduit as the scaffold, in an attempt to maintain the local microenvironment, block the invasion of fibrous connective tissue, and promote axonal growth. BMSCs have the potential to self-proliferate and differentiate into multiple cell types, and are seed cells for tissue engineering. Because of the difference in growth characteristics of BMSCs and fibroblasts, we purified and subcultured BMSCs for transplantation. Spinal cord injury models are often established by complete spinal cord transection, but such techniques have a high mortality rate (Basso et al., 2002). Here, we performed partial spinal cord transection and produced the same extent of spinal cord injury as traditional methods. Our method therefore eliminated common variables that arise using other spinal cord injury model methods, such as weight-drop, compression, and radiofrequency electrode impairment. In addition, our method did not require specialized equipment or techniques. We adopted a surgical repair

pattern for spinal cord hemisection injury and three kinds of intervention to observe histological differences between the three groups.

The results of the present study showed that after repair of spinal cord hemisection injury with a biological chitin conduit combined with BMSCs, the spinal cord retained its tubiform shape until 14 weeks. The majority of sleeve conduits in our study had degraded by this time, indicating that the conduit in the spinal cord is fully biocompatible. BMSCs within the conduits were growing well, indicative of their biocompatibility with stem cells and spinal cord tissue. The biological chitin conduit may improve the local microenvironment at the spinal cord injury site, effectively reduce the extent of the cavity, degeneration and necrosis, reduce glial scarring, and promote nerve regeneration, consistent with previous findings (Guest et al., 1997).

In the BCT and BCT + BMSC groups, local cavity formation and glial scarring were greatly reduced, and spinal cord myelin appeared to show good regeneration. Retrograde tracing revealed that nerve fibers at the distal and proximal ends of the injury site were connected to each other during nerve regeneration. There were more positive cells in the anterior horn of the spinal cord in the BCT group than in the injury group at 14 weeks post-injury, indicating that the biological conduit effectively promoted nerve fiber regeneration after spinal cord injury. At 8 weeks, the transplanted BMSCs survived and differentiated into Schwann-like cells expressing GFAP and S100, indicating that Schwann-like cells have the potential to promote nerve fiber regeneration in the spinal cord.

In the BCT group, GFAP-positive cells were not observed in the central injury area, but showed a symmetrical distribution at the distal and proximal ends. This distribution pattern indicates that astrocytes did not migrate into the central injury area, resulting in little glial scarring, whereas the local microenvironment at the distal and proximal ends was destroyed, leading to glial scar formation at the edge of the injury site. As the distance from the injury site increased, the impact on the microenvironment decreased, and permanent glial scar formation was gradually reduced.

In the BCT + BMSC group, BMSCs migrated after spinal cord injury, from the distal to the proximal end of injury, and from lateral to central. Currently, the mechanism underlying the role of BMSCs in the treatment of spinal cord injury remains unclear. Chopp and Li (2002) showed that inflammatory chemokines, cytokines and ischemic brain tissue contribute to the migration of BMSCs toward the ischemic lesion, and inflammatory cells that accumulate at the injury site also lead to migration. BMSCs differentiate into neurons and glial cells under appropriate environmental conditions, and nerve cells repair the structure of the injured spinal cord, thus recovering the connections between the nerves in the damaged nerve pathways (Cui et al., 2014). The implanted BMSCs interact with surrounding nerve tissue and generate some cytokines, such as polypeptides, neurotrophic factors, interleukins, macrophage colony-stimulating factor and stem cell factor. These cytokines not only

promote the restoration of neurological function, but also maintain the survival, proliferation, and migration of implanted BMSCs; BMSCs have the potential to differentiate into vascular endothelial progenitor cells and nerve cells, conducive to repairing damaged nerves and blood vessels (Neirinckx et al., 2014).

In summary, biological conduits combined with BMSCs significantly improve the local microenvironment and promote nerve fiber regeneration after spinal cord hemisection injury. The conduits provide a microenvironment conducive to BMSC proliferation, migration and differentiation in the spinal cord, protect neurons and promote axonal growth, effectively preventing the invasion of scar tissue. The transplanted BMSCs survive and differentiate into Schwann-like cells, thus promoting nerve regeneration.

**Author contributions:** *LYA and FX implemented the experiments. EJW provided experimental data. PXZ, YHK, and NH conceived and designed the study. YHK analyzed experimental data. FX drafted the manuscript. PXZ supervised the manuscript. XFY was responsible for statistical analysis. PXZ and XFY were responsible for the funds. NH provided technical or information support, and revised the study. All authors approved the final version of the manuscript.*

**Conflicts of interest:** *None declared.*

## References

- Basso DM, Beattie MS, Bresnahan JC (2002) Descending systems contributing to locomotor recovery after mild or moderate spinal cord injury in rats: experimental evidence and a review of literature. *Restor Neurol Neurosci* 20(5):189-218.
- Chopp M, Li Y (2002) Treatment of neural injury with marrow stromal cells. *Lancet Neurol* 1:92-100.
- Cui B, Li E, Yang B, Wang B (2014) Human umbilical cord blood-derived mesenchymal stem cell transplantation for the treatment of spinal cord injury. *Exp Ther Med* 7:1233-1236.
- Guest JD, Rao A, Olson L, Bunge MB, Bunge RP (1997) The ability of human Schwann cell grafts to promote regeneration in the transected nude rat spinal cord. *Exp Neurol* 148:502-522.
- Hyatt AJ, Wang D, van Oterendorp C, Fawcett JW, Martin KR (2014) Mesenchymal stromal cells integrate and form longitudinally-aligned layers when delivered to injured spinal cord via a novel fibrin scaffold. *Neurosci Lett* 569:12-17.
- Jia Y, Wu D, Zhang R, Shuang W, Sun J, Hao H, An Q, Liu Q (2014) Bone marrow-derived mesenchymal stem cells expressing the Shh transgene promotes functional recovery after spinal cord injury in rats. *Neurosci Lett* 573:46-51.
- Liu SF, Li CS, Xing Y, Tao F (2014) Effect of microenvironment modulation on stem cell therapy for spinal cord injury pain. *Neural Regen Res* 9:458-459.
- Lu P, Jones LL, Snyder EY, Tuszynski MH (2003) Neural stem cells constitutively secrete neurotrophic factors and promote extensive host axonal growth after spinal cord injury. *Exp Neurol* 181:115-129.
- Mohammadian M, Shamsasenjan K, Lotfi Nezhad P, Talebi M, Jahedi M, Nickkhab H, Minayi N, Movassagh Pour A (2013) Mesenchymal stem cells: new aspect in cell-based regenerative therapy. *Adv Pharm Bull* 3:433-437.
- Neirinckx V, Cantinieaux D, Coste C, Rogister B, Franzen R, Wislet-Gendebien S (2014) Concise review: Spinal cord injuries: how could adult mesenchymal and neural crest stem cells take up the challenge? *Stem cells* 32:829-843.
- Oliveri RS, Bello S, Biering-Sorensen F (2014) Mesenchymal stem cells improve locomotor recovery in traumatic spinal cord injury: systematic review with meta-analyses of rat models. *Neurobiol Dis* 62:338-353.
- Patist CM, Mulder MB, Gautier SE, Maquet V, Jerome R, Oudega M (2004) Freeze-dried poly(D,L-lactic acid) macroporous guidance scaffolds impregnated with brain-derived neurotrophic factor in the transected adult rat thoracic spinal cord. *Biomaterials* 25:1569-1582.
- Sundback C, Hadlock T, Cheney M, Vacanti J (2003). Manufacture of porous polymer nerve conduits by a novel low-pressure injection molding process. *Biomaterials* 24:819-830.
- Teng YD, Lavik EB, Qu X, Park KI, Ourednik J, Zurakowski D, Langer R, Snyder EY (2002) Functional recovery following traumatic spinal cord injury mediated by a unique polymer scaffold seeded with neural stem cells. *Proc Natl Acad Sci USA* 99:3024-3029.
- Tsai EC, Dalton PD, Shoichet MS, Tator CH (2004) Synthetic hydrogel guidance channels facilitate regeneration of adult rat brainstem motor axons after complete spinal cord transection. *J Neurotrauma* 21:789-804.
- Yin F, Guo L, Meng CY, Liu YJ, Lu RF, Li P, Zhou YB (2014) Transplantation of mesenchymal stem cells exerts anti-apoptotic effects in adult rats after spinal cord ischemia-reperfusion injury. *Brain Res* 1561:1-10.
- Zhang P, He X, Zhao F, Zhang D, Fu Z, Jiang B (2005) Bridging small-gap peripheral nerve defects using biodegradable chitin conduits with cultured schwann and bone marrow stromal cells in rats. *J Reconstr Microsurg* 21:565-571.
- Zhang P, Yin X, Kou Y, Wang Y, Zhang H, Jiang B (2008) The electrophysiology analysis of biological conduit sleeve bridging rhesus monkey median nerve injury with small gap. *Artif Cells Blood Substit Immobil Biotechnol* 36:457-463.
- Zhang P, Zhang C, Kou Y, Yin X, Zhang H, Jiang B (2009) The histological analysis of biological conduit sleeve bridging rhesus monkey median nerve injury with small gap. *Artif Cells Blood Substit Immobil Biotechnol* 37:101-104.
- Zhang P, Kou Y, Yin X, Wang Y, Zhang H, Jiang B (2011) The experimental research of nerve fibers compensation amplification innervation of ulnar nerve and musculocutaneous nerve in rhesus monkeys. *Artif Cells Blood Substit Immobil Biotechnol* 39:39-43.
- Zhang P, Han N, Wang T, Xue F, Kou Y, Wang Y, Yin X, Lu L, Tian G, Gong X, Chen S, Dang Y, Peng J, Jiang B (2013) Biodegradable conduit small gap tubulization for peripheral nerve mutilation: a substitute for traditional epineurial neuroorrhaphy. *Int J Med Sci* 10:171-175.
- Zhang ZC, Li F, Sun TS (2013) Spinal cord injury and neural regeneration: an expert consensus on the evaluation and treatment of acute thoracolumbar spine and spinal cord. *Neural Regen Res* 8:3077-3086.

*Copypedited by Murphy JS, Norman C, Wang J, Yang Y, Li CH, Song LP, Zhao M*